Journal of Nuclear Materials 434 (2013) 395–401

Contents lists available at SciVerse ScienceDirect

Journal of Nuclear Materials

journal homepage: www.elsevier.com/locate/jnucmat

Hydrogen behaviors in molybdenum and tungsten and a generic vacancy trapping mechanism for H bubble formation

Lu Sun, Shuo Jin *, Xiao-Chun Li, Ying Zhang, Guang-Hong Lu *

Department of Physics, Beihang University, Beijing 100191, China

ARTICLE INFO

Article history:
Received 10 August 2012
Accepted 5 December 2012
Available online 14 December 2012

ABSTRACT

We investigate the trapping behaviors of hydrogen (H) in molybdenum (Mo) and tungsten (W) using a first-principles method with a zero point energy correction as well as the molecular dynamics (MD) method. The H trapping is found to generally satisfy the "optimal charge density" rule at the vacancy, and a monovacancy is shown to simultaneously trap 14 H with a H_2 molecule formed at the vacancy center in both Mo and W. On the other hand, the MD simulation shows the temperature decreases the number of trapped H at the vacancy. We further propose a generic vacancy trapping mechanism for H bubble formation in metals. The H atoms will first saturate the internal surface of the vacancy (or other vacancy-type defects) to form a "screening layer", which can screen the interaction between the further trapped H and the surrounding metal atoms. This leads to the formation of H_2 molecule at the vacancy center, which can be considered as the preliminary stage of H bubble nucleation.

1. Introduction

In the future magnetic confinement fusion reactors, plasma facing materials (PFMs) should withstand irradiation from low energy (0–100 eV) and high-flux (>10^{24}/m^2s) plasma of hydrogen (H) isotopes and helium (He) as well as neutrons with the energy of 14.2 MeV and high heat flux from several MW/m^2 to several hundred MW/m^2 [1–4]. This requires PFMs to retain the structure integrity even at high temperature of 900 °C [5]. Consequently, the properties as well as choices of PFMs have an important influence on the success of the future magnetic confinement fusion reactors [6]. High-Z metal tungsten (W) and molybdenum (Mo) are both refractory metals with good thermal properties, low sputtering erosion and low H isotope retention [7–9]. W and W alloys are now considered as the most promising candidates for PFMs [10–12], which are already successfully used in the ASDEX-U tokamak [13]. While Mo and Mo alloys are deemed as another potential PFM candidate [7–9,14], which are being used in the Alcator C-Mod tokamak [14–16]. W has higher melting point and higher threshold for sputtering than Mo, which leads to a better radiation resistance of W but the high temperature embrittlement of W limits its application as PFM [7,8,17]. On the other hand, Mo has lower melting point which, however, makes it more easily be shaped due to its better ductility than W [7–9].

Mo and W based PFMs will be exposed to low energy (0–100 eV) and high-flux (>10^{24}/m^2s) H-isotope plasma [1,2], and the accumulation of H in PFMs can cause H bubble formation and blistering [11,12,18], decreasing mechanical properties of PFMs [1]. H retention in Mo and W is closely related to the H blistering, making H retention a crucial subject [14,18]. H isotope retention in both Mo and W is a rather complicate issue depending on different experimental conditions [7,9,19–21]. Temperature is an important factor in determining the retained H isotopes, and totally diverse results have been obtained in Mo and W at different temperatures. For example, the fractional D retention is lower in Mo than that in W at 600 K under the tritium plasma experiment [9], while it is lower in W at above 700 K according to the depth profile [19,20]. On the other hand, the incident ion fluence is another important factor to affect the amounts of H isotopes retained in both Mo and W. The H isotope retention was found to reach saturation with increasing ion fluence in W, which was not found in Mo, however, until fluence of ~10^{25} m^{-2} [21]. Moreover, parameters such as diffusivity and recombination coefficient directly determine the dynamic H retention behavior in metals [14,18,21,22]. The H isotopes exhibit high diffusivity, low solubility and high recombination coefficient in both Mo and W which are strongly temperature dependent, leading to the low H isotope retention that is expected during the operation of a fusion reactor [7,14,22–25].

The retention behavior of H (as well as its isotopes) is closely associated with the trapping process of H by defects such as vacancy, grain boundary and dislocation in metals. It has been experimentally proved that H isotopes have a strong interaction with the vacancy and can be trapped by the vacancy clusters in both Mo and W [19,20,26]. The microscopic scale trapping behaviors of H at the vacancy in W have been examined by series of theoretical works, which also demonstrate the vacancy serves as a trapping center

* Corresponding authors. Tel./fax: +86 (10) 82339917.
E-mail addresses: jinshuo@buaa.edu.cn (S. Jin), LGH@buaa.edu.cn (G.-H. Lu).

0022-3115/$ - see front matter © 2012 Elsevier B.V. All rights reserved.
http://dx.doi.org/10.1016/j.jnucmat.2012.12.008

for H atoms [27–30]. Liu et al. [27] first proposed that H will bind onto an isosurface of optimal charge density inside the W monovacancy, and the H_2 molecule forms at the center of vacancy when 10 H atoms are embedded. Johnson et al. [28] then considered the zero point energy (ZPE) correction to the trapping energy of H at the vacancy in W, showing at least 6 H atoms could be trapped by a monovacancy. In the work of Ohsawa et al. [29], more accurate configurations of multi-H at a monovacancy have been determined which shows 14 H atoms can be trapped by one monovacancy. Zhou et al. gave the number of H that can be trapped at the W grain boundary associated with the optimal charge density, and proposed the H bubble formation at the grain boundary should be via a vacancy trapping mechanism [12]. On the other hand, by thermodynamic estimation, Heinola et al. [30] took the temperature effect into account on the trapping behavior of H in W, and predicted the W monovacancy could hold up to only 5 H at room temperature.

In this paper, upon the summarization of previous results, we first give a more detailed analysis of the H trapping behaviors in both Mo and W with ZPE corrections, particularly the optimal charge density of H at the vacancy. Further, we employ the molecular dynamics (MD) simulation to show the numbers and configurations of H at the vacancy that are temperature dependent in comparison with those from the first-principles. Finally, we propose a generic vacancy trapping mechanism of H in metals, which has already been elucidated in our previous work [27]. This will be much helpful for understanding the H retention and bubble formation in Mo and W as well as other metals and alloys.

2. Methodology

First-principles calculations are performed using the pseudopotential plane wave method implemented in the Vienna ab initio simulation package (VASP) code [31,32] based on the density-functional theory. We use the generalized gradient approximation of Perdew and Wang [33] and projector augmented wave potentials [34] with a plane wave energy cutoff of 350 eV. The bcc Mo supercell and W supercell of 128 atoms containing a monovacancy are adopted. The Brillouin zone is sampled with $3 \times 3 \times 3$ k-points by the Monkhorst–Pack scheme [35]. The calculated equilibrium lattice constant is 3.154 Å for Mo and 3.172 Å for W, in good agreement with the experimental values of 3.15 Å for Mo and 3.16 Å for W. Both supercell size and atomic positions are relaxed to equilibrium, and energy minimization is converged until the forces on all atoms are less than 10^{-3} eV Å^{-1}.

In the MD simulations, we employ self-developed interatomic potentials based on an analytical bond-order scheme for a W–H system [36]. All of the simulations are performed with the MD code LAMMPS [37]. The simulation box size was $10a \times 10a \times 10a$, where a is the lattice constant of bcc W, with the constant pressure and the periodic boundary condition. The Polak–Ribiere version of the conjugate gradient (CG) algorithm is employed to make the relaxations, and the stopping tolerances for energy and force are 10^{-9} eV and 10^{-9} eV Å^{-1}, respectively. The variable time step algorithm varies from 0.05 *fs* to 1 *fs*, and the maximum distance for an atom to move in one time step is 0.2 Å. Temperature and pressure are controlled using the Nose–Hoover thermostat and barostat [38,39].

3. Results and discussion

3.1. Configurations and optimal charge density of H at the vacancy

Since the ZPE of H has not been taken into account in all the previous calculations of the H behaviors in Mo, we first calculate the energies of H in Mo with ZPE corrections. The ZPE is the energy of vibration of the molecule at temperature of absolute zero (T = 0 K), and as a light element, the ZPE of H cannot be neglected [40]. ZPE of H is calculated from the Hessian matrix by allowing only the harmonic vibration for H [30,41]. Without considering the ZPE, single H is shown to prefer to occupy the tetrahedral interstitial site (TIS) with a formation energy of 0.62 eV in intrinsic Mo [24] in comparison with 0.94 eV at the octahedral interstitial site (OIS). With considering the ZPE, the formation energies of H at the TIS and the OIS are 0.87 eV and 1.16 eV with the ZPE corrections of 0.25 eV and 0.22 eV, respectively. The TIS is still the most energetically stable site for H in Mo, and the positive values of formation energy suggest that the dissolution of H in Mo is an endothermic process.

In the previous work, we elucidate that the trapping energy (the embedding energy) of H in W depends largely on the electron density [27]. However, the electron density in the bulk W is much higher than the optimal density for H determined by the homogeneous electron gas model [42,43]. In order to further lower the H trapping energy, it is desirable to create a structure that can decrease the electron density, and the vacancy can lower such electron density in its vicinity by providing an effective mechanism to meet this requirement. For Mo as a transition metal with the same subgroup as W, it is similar that vacancy should be taken into account since it can lower the electron density and thus decrease the trapping energy.

At a monovacancy in Mo, present calculations show that single H atom occupies a position of ~1.23 Å off the vacancy center close to an OIS with a formation energy of −0.24 eV with the ZPE correction, indicating that H can be easily trapped with the presence of vacancy, different from the positive formation energy of H at the interstitial sites. Similar to the W case, H occupation in Mo also satisfies the rule of "optimal charge density" [12,27]. Seen from Fig. 1, H prefers to bind onto an isosurface of the same charge density which is 0.10 electron Å^{-3} surrounding the vacancy in Mo. According to such "optimal charge density" rule, we are able to bring H atom one by one into the vacancy, and minimize the energy to find the optimal-embedding site each step and determine the atomic configurations of multi-H atoms in Mo. Each H is placed on the isosurface of optimal charge density shown in Fig. 1.

With increasing number of H at the vacancy, the isosurface of optimal charge density for H occupation shrinks, as shown in Fig. 2, indicating less available "optimal charge density" sites that the vacancy can accommodate for H. This makes it more difficult for H to be trapped by the vacancy. The occupation of H is shown to be close to the OIS first at the number range of 1–6, while it is close to TIS starting from the 7th H with 2 H atoms on one internal surface of vacancy until the 12th H, at which the isosurface of optimal charge density completely shrinks to the vacancy center. Further H atoms thus have to occupy the vacancy center. Seen from Fig. 3n, when the 14th H atom is embedded into the vacancy, the distance of 2 H atoms at the center of the vacancy is ~0.74 Å, close

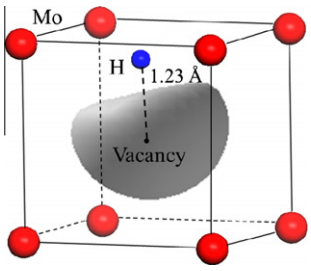

Fig. 1. Occupancy of single H at the vacancy in Mo and isosurface of the optimal charge density of H.

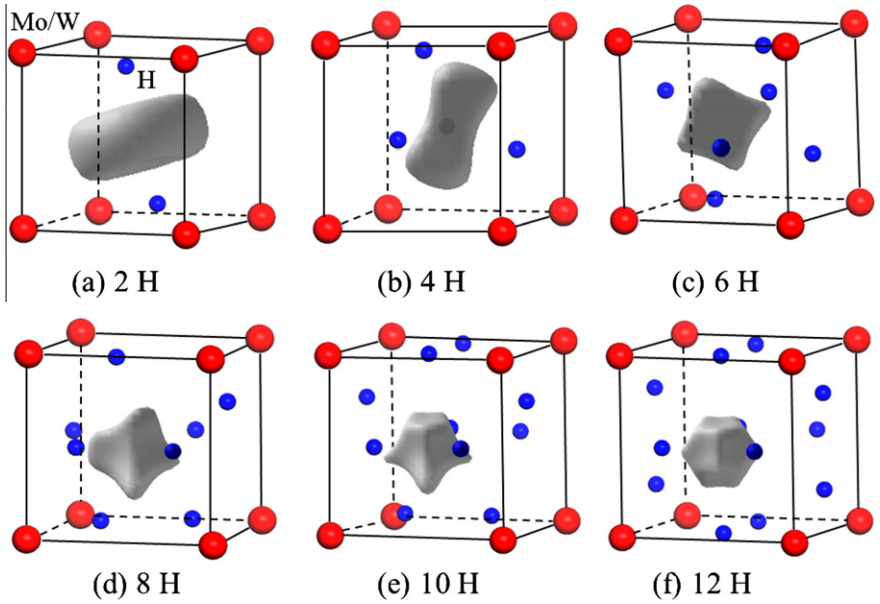

Fig. 2. Evolution of the optimal charge density isosurface with increasing number of H at the vacancy in Mo/W.

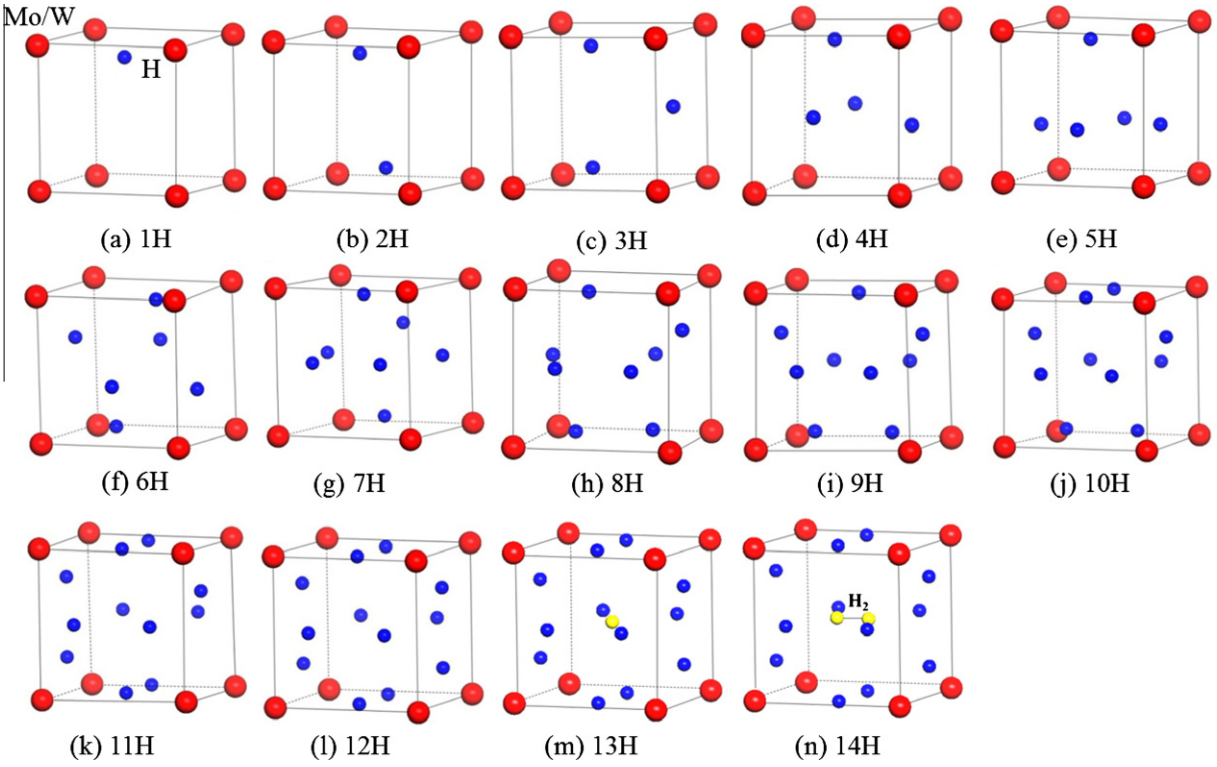

Fig. 3. Atomic configurations for H (from 1 to 14) at the vacancy in Mo and W.

to the bond length of the H_2 molecule (0.75 Å), implying that the H_2 molecule forms at the vacancy center.

W exhibits the same bcc crystal structure as Mo with almost the same lattice constant (3.17 Å vs. 3.15 Å). Also, both W and Mo are in the same subgroup *VI* with exactly the same number of valence electrons. Therefore, the atomic configurations and evolution of the optimal charge density isosurface for multi-H occupation at the vacancy in W are shown to be the same as those in Mo, as shown in Figs. 2 and 3, respectively. However, the trapping energies of H at the vacancy in W and Mo are different, as discussed in the following.

3.2. Trapping energy of H at the vacancy

We calculate the trapping energies of H at the vacancy in Mo as well as in W for a comparison corresponding to the configurations shown above, based on which we can determine the maximum number of H that one vacancy can hold up. There are two ways for the trapping process of H in Mo and W, which only differ in their definitions but share the same H positions and total energies. One is "the simultaneous way", i.e., multi-H atoms dissolve into the vacancy at the same time, for which the average trapping energy (E_{sim}^{trap}) per H can be obtained by

$$E_{sim}^{trap} = \frac{1}{n}[E_{(N-1)Mo(W),V,nH} - E_{(N-1)Mo(W),V}] - [E_{NMo(W),H_{TIS}} - E_{NMo(W)}], \quad (1)$$

where $E_{(N-1)Mo(W),V,nH}$ and $E_{(N-1)Mo(W),V}$ are total energies of supercell containing $(N-1)$ Mo (W) atoms and a monovacancy with n H atoms and without H, and $E_{NMo(W),H_{TIS}}$ and $E_{NMo(W)}$ are energies of intrinsic Mo (W) supercell with a tetrahedral H and without H, respectively. Another way for H trapping is "the sequential way", i.e., multi-H atoms dissolve into the vacancy one by one, for which the trapping energy (E_{seq}^{trap}) per H can be obtained by

$$E_{seq}^{trap} = E_{(N-1)Mo(W),V,nH} - E_{(N-1)Mo(W),V,(n-1)H} - E_{NMo(W),H_{TIS}} + E_{NMo(W)}, \quad (2)$$

Based on Eqs. (1) and (2), H trapping energy is found to be as a function of the number of H dissolved in the vacancy in Mo and W for both the simultaneous way and the sequential way, as shown in Figs. 4 and 5, respectively. The trapping energy can be understood as the gained energy when H is added into the vacancy, and the negative value means exothermic. Without ZPE corrections, the first H is embedded into the vacancy in Mo and W with a trapping energy of −1.02 eV and −1.20 eV, respectively, with the reference energy as the energy of H at TIS far away from the vacancy. This suggests a strong attraction between H and the vacancy. The lower trapping energy of H indicates the vacancy can accommodate more H atoms in both Mo and W. Since the trapping energy in W is ~0.2 eV lower than that in Mo, the vacancy in W should trap more H atoms from the energy point of view. This may explain the experimentally observed lower H retention in Mo in comparison with W [7,9,19–22].

For the simultaneous way, with more H going into the vacancy, the trapping energy increases in both Mo and W (Fig. 4), indicating the number of H that the vacancy can accommodate becomes less. Overall, the trapping energy of H in W is ~0.2 eV lower than that in Mo. For both Mo and W, an obvious rise of the trapping energy is observed when the 13th H atom is embedded in the vacancy center (Fig. 3m). The energy is then reduced due to the coming of 14th H, which bonds to the 13th H to form a H_2 molecule at the vacancy center (Fig. 3n). Therefore, the vacancy can accommodate up to 14 H in both Mo and W for the simultaneous way based on the first-principles simulations. The trapping energy is still negative, indicating the possibility that more H atoms can be trapped. This can be confirmed by the MD simulations (see Section 3.3).

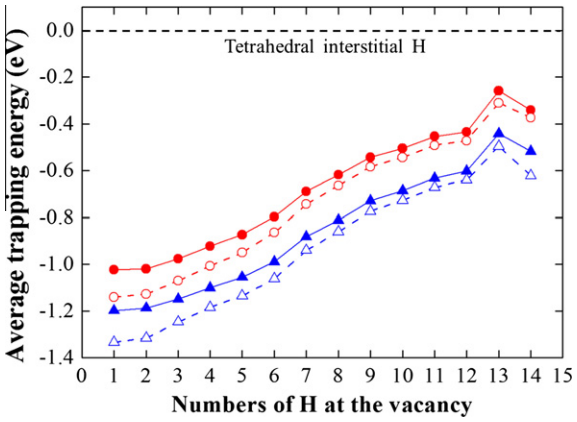

Fig. 4. Average trapping energy vs. the numbers of H at the vacancy in Mo (red solid circles) and W (blue solid triangles) for the simultaneous way. The red hollow circles and the blue hollow triangles represent the trapping energy with the ZPE corrections in Mo and W, respectively. (For interpretation of the references to color in this figure legend, the reader is referred to the web version of this article.)

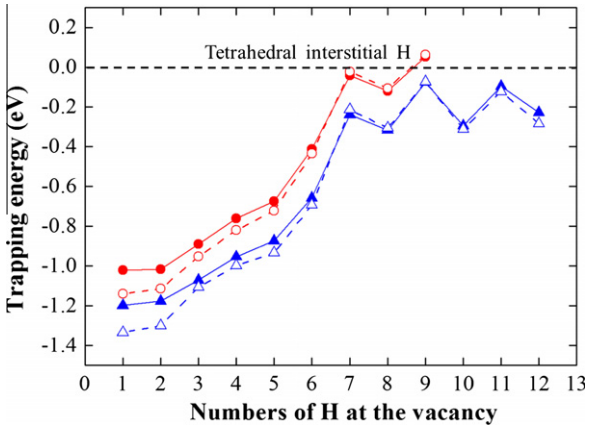

Fig. 5. The trapping energy vs. the numbers of H at the vacancy in Mo (red solid circles) and W (blue solid triangles) for the sequential way. The red hollow circles and the blue hollow triangles represent the trapping energy with the ZPE corrections in Mo and W, respectively. (For interpretation of the references to color in this figure legend, the reader is referred to the web version of this article.)

Similar to the simultaneous way, the trapping energy for the sequential way is also increases with increasing H number, as shown in Fig. 5. The absolute value of trapping energy is, however, higher than that for the simultaneous way for each number of trapped H atoms in both Mo and W. Different from the simultaneous way, it can be observed for the sequential way that the vacancy in Mo can trap 8 H at most because the trapping energy of the 9th H becomes positive (+0.05 eV), higher than the reference energy at TIS, while at least 12 H can be trapped by the vacancy in W. Moreover, for all the number of H at the vacancy, the H trapping energy in Mo is shown to be ~0.2 eV higher as compared with that in W, similar to the simultaneous way.

The main reason of the different numbers of H trapped by the vacancy for the two trapping ways relies on different mechanisms based on their different definitions. For the simultaneous way, n H atoms are fitted at an empty vacancy, forming nH-vacancy complex as a result. For the sequential way, further H is trapped by the $(n-1)$H-vacancy complex to form nH-vacancy complex. The H atoms previously trapped by the vacancy can prevent the trapping of further H for the sequential way, while the empty vacancy would have a larger capacity to hold more H atoms simultaneously.

We further consider the H trapping energies at the vacancy with the ZPE corrections, as shown in Figs. 4 and 5. The calculated ZPE increases with increasing number of trapped H atoms as list in Table 1. The ZPE correction generally leads to a lower trapping energy. For example, the ZPE of the first H is calculated to be 0.14 eV and 0.13 eV, resulting in the trapping energy of −1.14 eV and −1.20 eV in comparison with −1.02 eV and −1.33 eV without the ZPE correction in Mo and W, respectively. The ZPE only changes the absolute value of the trapping energy, but does not change the energy variation trend as well as the number of H atoms that the vacancy can accommodate. For example, the maximum number of H that is sequentially captured by the vacancy remains to be 8 in Mo, with a positive trapping energy for the 9th H which is +0.06 eV with ZPE correction. Also, the vacancy can still trap 12 H sequentially in W with ZPE correction.

3.3. Molecular dynamics simulation on H trapping behavior

In first-principles calculations, a detailed analysis has been given on the occupation and trapping behaviors of H at the vacancy in Mo as well as W. However, the first principles method can only simulate the ground state at 0 K with a supercell generally containing no more than 200 atoms. More configurations of trapping H at

Table 1
Calculated ZPE of trapped multi-H atoms at the vacancy in Mo and W (eV).

*n*H	1	2	3	4	5	6	7	8	9	10	11	12	13	14
Mo	0.14	0.29	0.48	0.68	0.88	1.11	1.39	1.65	1.92	2.15	2.37	2.59	2.61	3.08
W	0.13	0.27	0.50	0.71	0.92	1.15	1.43	1.71	1.97	2.22	2.46	2.69	2.71	3.23

the vacancy as well as the temperature effect can be taken into account in the MD simulation. Particularly, temperature is shown to have an important effect on the H behavior at the vacancy [9,14,30].

By the MD simulation, the trapping energy of H as a function of number of trapped H at the vacancy in W is provided (the simultaneous way). As shown in Fig. 6, the trapping energy increases as trapped H number rises. With the energy of H at the TIS as the reference energy, the vacancy in W can trap as many as 20 H atoms, more than 14 H from the first-principles calculation (Fig. 4). The most energetically favorable configurations corresponding to different numbers of trapped H atoms are determined from as many as several hundred possible configurations, as shown in Fig. 7. As a matter fact, most of the configurations are more or less different from those determined from the first principles. It should be mentioned that 12 H atoms are found to form a stable icosahedron at the vacancy, which is quite similar to the first-principles results (Fig. 3), and also the same as the 12 H atoms case with He at the vacancy center in W [43].

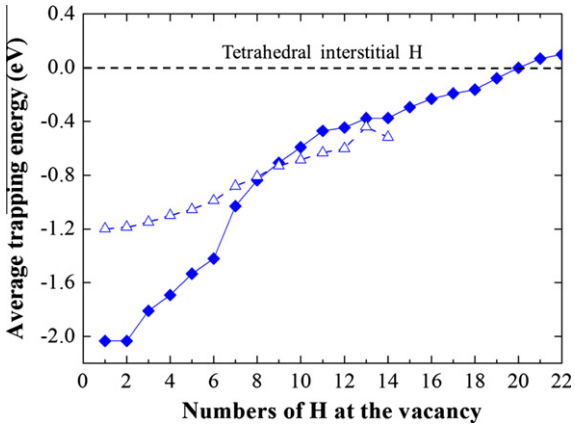

Fig. 6. Average trapping energy vs. the numbers of H at the vacancy in W at 0 K from the MD simulations (bule solid diamonds) in comparison with the first-principles simulations (blue hollow triangles). (For interpretation of the references to color in this figure legend, the reader is referred to the web version of this article.)

The H_2 molecule forms when more H atoms are embedded in the vacancy (larger than 12), as shown in Figs. 7m and n, basically consistent with the first principles results. With number of trapped H more than 12, H atom will not stay inside the vacancy any more, but occupy the sites surrounding the vacancy (not shown in Fig. 7) with lower trapping energy in comparison with the TIS. These results have not given by the first-principles calculations due to much more computational time. However, it can be predicted from the trapping energy results (Fig. 4) because the trapping energy for the 14 H case is still much lower (~0.6 eV) than that at the TIS.

Next, we investigate the effect of temperature on the H trapping behavior in W, particularly the number of H that one vacancy can hold up. We make a statistical average to evaluate the H numbers trapped at the vacancy at different temperatures. Fig. 8 shows the number of trapped H at the vacancy in W decreases with the increasing temperature, suggesting that temperature weakens

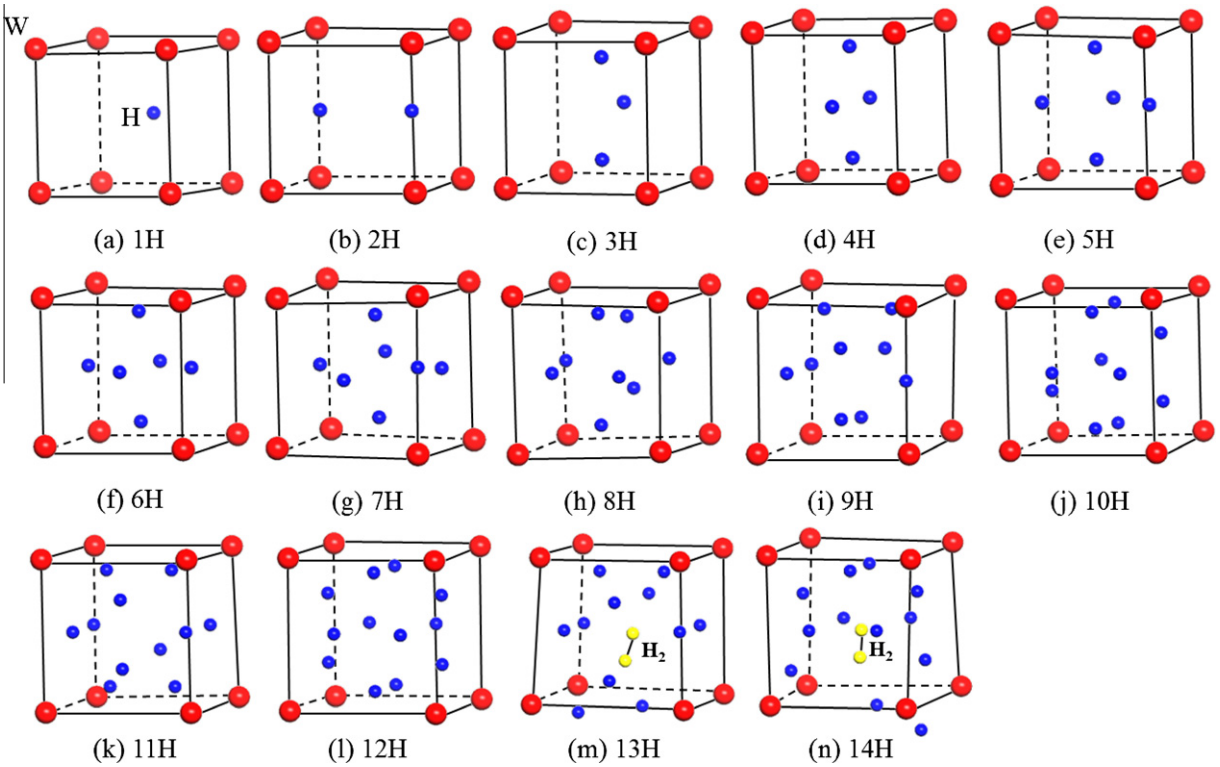

Fig. 7. Atomic configurations for multi-H at the vacancy in W at 0 K determined via the MD simulations.

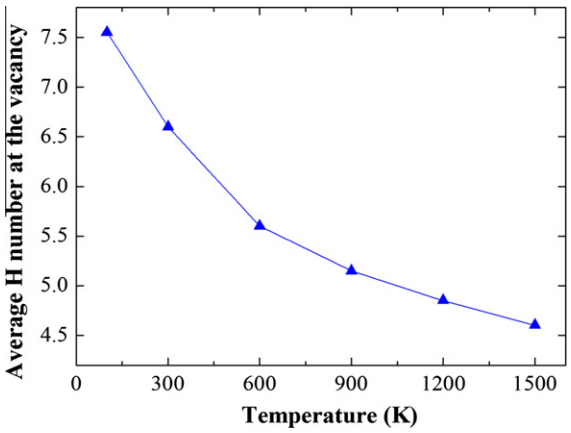

Fig. 8. Average trapped H number at the vacancy as a function of the temperature in W from the MD simulations.

the H trapping capacity of vacancy. At temperature of 300 K, only ~6.5 H atoms can be trapped by a monovacancy, while it decreases to ~5 H at 900 K. This confirms that the thermodynamic estimation on the number of trapped H atoms at the vacancy in W is basically correct, which gave 5 H at the room temperature [30]. The accurate number as well as the corresponding configurations at 0 K determined by the previous work [27–29] may be not so important, because temperature will largely decrease the number of H atoms that can be trapped by the vacancy and alter the configurations.

3.4. Vacancy trapping mechanism for H bubble formation in metals

According to all the results above, we are able to propose a vacancy trapping mechanism for H bubble formation in Mo and W, which has been already suggested in our previous work [12,27]. As schematically shown in Fig. 9, vacancy (or vacancy cluster, and even a void) can provide an isosurface of the optimal charge density for H, and thus lower the energy of H, making H be able to be trapped by the vacancy in Mo or W. H thus prefers to occupy the internal surface of the vacancy instead of the vacancy center due to the H–W interaction. (In comparison, He with a close shell structure will occupy the vacancy center with the lowest charge density because the optimal charge density for He is zero [44].) With H continuously diffusing in, H atoms will saturate the internal surface of the vacancy to form a "screening layer", which can partly screen the interaction between the further trapped H atoms and the surrounding Mo/W atoms, making these H atoms go into the vacancy center. This leads to the formation of H_2 molecule at the vacancy center finally, which can be considered as the preliminary stage of H bubble nucleation.

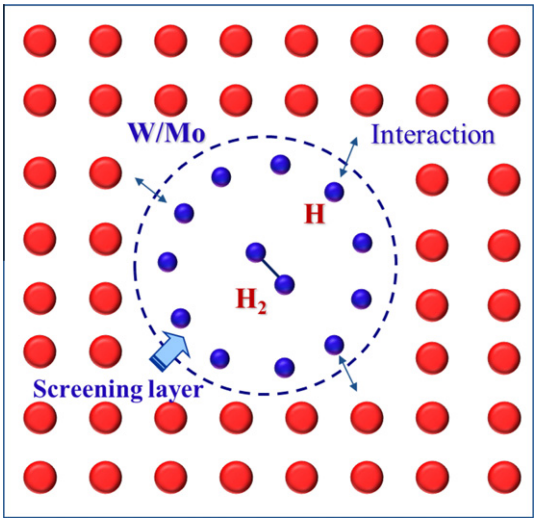

Fig. 9. Vacancy trapping mechanism for H bubble formation in metals.

H_2 molecule is proved to form at the vacancy center in Mo and W at 0 K based on the vacancy trapping mechanism. It can be predicted that more H_2 molecules can form at vacancy clusters or voids with more space for H to stay. According to the mechanism of optimal charge density, the trapping energy of H at a vacancy cluster or a void with a larger space should be lower because such large space can provide lower charge density which is more optimal for H. This suggests that the vacancy clusters with larger space can trap more H, and thus have more H_2 molecules formed in the center. For example, the trapping energy of one H atom at a divacancy in W is calculated by first-principles to be −1.36 eV, lower than the trapping energy of −1.20 eV at a monovacancy, and two H_2 molecules can form at the center of the divacancy [27]. Further, the experimental work reported that H can be more easily trapped at the inner wall of a void with a trapping energy of −1.71 eV in W, lower than −0.95 eV for H trapped at a single vacancy [45]. Therefore, at certain temperature, the H_2 molecule can form only when the vacancy or the vacancy cluster is large enough. Namely, these exists a critical size of the vacancy that is needed for the formation of the H_2 molecule. This is on the investigation via the MD simulation.

We note that such vacancy trapping mechanism for H bubble formation in Mo and W is generic, and can also be expected to be applied to other metals and alloys [27]. Further, the mechanism can be also applied to any other vacancy-type defects that can provide enough space to accommodate H, leading to the H_2 molecule formation. Experimental works have demonstrated that the dissolved H atoms can be easily trapped by those vacancy-type defects including vacancy-clusters or voids [46,47], grain boundaries [18] and dislocations [48], and H will accumulate and finally form H bubble in these defects. The present vacancy trapping mechanism can well explain these experimental results.

4. Conclusions

Using a first-principles method, we investigate the trapping behaviors of H in Mo as well as W with the zero point energy correction. The H trapping is found to generally satisfy the "optimal charge density" rule at the vacancy, and the vacancy plays a crucial rule in the H trapping in Mo and W. Based on the trapping energies of H as a function of the number of trapped H, a monovacancy is shown to simultaneously trap 14 H with a H_2 molecule formed at the vacancy center in both Mo and W, while sequentially trap only 8 H in Mo and 12 H in W without the H_2 molecule formation. On the other hand, the MD simulation shows as many as 20 H can be trapped at a monovacancy in W, and the temperature decreases the number of H trapped at the vacancy. At temperature of 300 K, only ~6.5 H atoms can be trapped by a monovacancy in W, while it decreases to ~5 H without the formation of the H_2 molecule at 900 K.

Based on these results, we propose a vacancy trapping mechanism for H bubble formation in metals. Vacancy (or vacancy cluster, and even a void) can provide an isosurface of the optimal charge density for H, and thus H prefers to occupy the internal surface of the vacancy instead of the vacancy center. The so-trapped H atoms will saturate the internal surface of the vacancy to form a "screening layer", which can screen the interaction between the further trapped H atoms and the surrounding Mo/W atoms, making these H atoms go into the vacancy center. This leads to

the formation of H_2 molecule at the vacancy center finally, which can be considered as the preliminary stage of H bubble nucleation. Such mechanism is generic, and can be applied to other metals as well as any other vacancy-type defects such as grain boundary and dislocation.

Acknowledgement

This research is supported by the National Natural Science Foundation of China (NSFC) through Grant Nos. 51061130558 and 51001006.

References

[1] J.B. Condon, T.J. Schober, J. Nucl. Mater. 207 (1993) 1.
[2] G.N. Luo, W.M. Shu, M. Nishi, J. Nucl. Mater. 347 (2005) 111.
[3] R. Matera, G. Federici, J. Nucl. Mater. 233–237 (1996) 17.
[4] J. Linke, F. Escourbiac, I.V. Mazul, R. Nygren, M. Rödig, J. Schlosser, S. Suzuki, J. Nucl. Mater. 367–370 (2007) 1422.
[5] D.L. Smith, S. Majumdar, M. Billone, R. Mattas, J. Nucl. Mater. 283–287 (2000) 716.
[6] The fusion energy is being developed internationally via the ITER (International Thermonuclear Experimental Reactor) Project.
[7] O.V. Ogorodnikova, J. Nucl. Mater. 390–391 (2009) 651.
[8] R.A. Causey, C.L. Kunz, D.F. Cowgill, J. Nucl. Mater. 337–339 (2005) 600.
[9] J.P. Sharpe, R.D. Kolasinski, M. Shimada, P. Calderoni, R.A. Causey, J. Nucl. Mater. 390–391 (2009) 709.
[10] G. Janeschitz, J. Nucl. Mater. 290–293 (2001) 1.
[11] Y.L. Liu, Y. Zhang, G.N. Luo, G.H. Lu, J. Nucl. Mater. 390–391 (2009) 1032.
[12] H.B. Zhou, Y.L. Liu, S. Jin, Y. Zhang, G.N. Luo, G.H. Lu, Nucl. Fusion 50 (2010) 025016.
[13] H. Bolt, V. Barabash, W. Krauss, J. Linke, R. Neu, S. Suzuki, N. Yoshida, J. Nucl. Mater. 329–333 (2004) 66.
[14] G.M. Wright, D.G. Whyte, B. Lipschultz, J. Nucl. Mater. 390–391 (2009) 544.
[15] D.A. Pappas, B. Lipschultz, B. LaBombard, M.J. May, C.S. Pitcher, J. Nucl. Mater. 266–269 (1999) 635.
[16] W.R. Wampler, B. LaBombard, B. Lipschultz, G.M. McCracken, D.A. Pappas, C.S. Pitcher, J. Nucl. Mater. 266–269 (1999) 217.
[17] C.H. Wu, U. Mszanowski, J. Nucl. Mater. 218 (1995) 293.
[18] R.A. Causey, J. Nucl. Mater. 300 (2002) 91.
[19] S. Nagata, K. Takahiro, J. Nucl. Mater. 283–287 (2000) 1038.
[20] S. Nagata, K. Takahiro, J. Nucl. Mater. 266–269 (1999) 1151.
[21] A.A. Haasz, J.W. Davis, J. Nucl. Mater. 241–243 (1997) 1076.
[22] E. Serra, G. Benamati, O.V. Ogorodnikova, J. Nucl. Mater. 255 (1998) 105.
[23] Y.L. Liu, S. Jin, L. Sun, C. Duan, Comput. Mater. Sci. 54 (2012) 32.
[24] C. Duan, Y.L. Liu, H.B. Zhou, Y. Zhang, S. Jin, G.H. Lu, G.N. Luo, J. Nucl. Mater. 404 (2010) 109.
[25] Y.L. Liu, H.B. Zhou, Y. Zhang, J. Alloys Compd. 509 (2011) 8277.
[26] H. Eleveld, A. vanVeen, J. Nucl. Mater. 191–194 (1992) 433.
[27] Y.L. Liu, Y. Zhang, H.B. Zhou, G.H. Lu, F. Liu, G.N. Luo, Phys. Rev. B 79 (2009) 172103.
[28] D.F. Johnson, E.A. Carter, J. Mater. Res. 25 (2010) 315.
[29] K. Ohsawa, J. Goto, M. Yamakami, M. Yamaguchi, M. Yagi, Phys. Rev. B 82 (2010) 184117.
[30] K. Heinola, T. Ahlgren, K. Nordlund, J. Keinonen, Phys. Rev. B 82 (2010) 094102.
[31] G. Kresse, J. Hafner, Phys. Rev. B 47 (1993) 558.
[32] G. Kresse, J. Furthmuller, Phys. Rev. B 54 (1996) 11169.
[33] J.P. Perdew, Y. Wang, Phys. Rev. B 45 (1992) 13244.
[34] P.E. Blochl, Phys. Rev. B 50 (1994) 17953.
[35] H.J. Monkhorst, J.D. Pack, Phys. Rev. B 13 (1976) 5188.
[36] X.C. Li, X.L. Shu, Y.N. Liu, F. Gao, G.H. Lu, J. Nucl. Mater. 408 (2011) 12.
[37] S.J. Plimpton, J. Comp. Phys. 117 (1995) 1.
[38] W.G. Hoover, A.J. Ladd, B. Moran, Phys. Rev. Lett. 48 (1982) 1818.
[39] S. Nose, Mol. Phys. 52 (1984) 255.
[40] B. Jiang, F.R. Wan, W.T. Geng, Phys. Rev. B 81 (2010) 134112.
[41] R. Matsumoto, Y. Inoue, S. Taketomi, N. Miyazaki, Scr. Mater. 60 (2009) 555.
[42] M.J. Puska, R.M. Nieminen, M. Manninen, Phys. Rev. B 24 (1981) 3037.
[43] J.K. Norskov, F. Besenbacher, J. Less Common Met. 130 (1987) 475.
[44] H.B. Zhou, Y.L. Liu, S. Jin, Y. Zhang, G.N. Luo, G.H. Lu, Nucl. Fusion 50 (2010) 115010.
[45] M. Poon, A.A. Haasz, J.W. Davis, J. Nucl. Mater. 374 (2008) 390.
[46] S.M. Myers, P.M. Richards, W.R. Wampler, J. Nucl. Mater. 165 (1989) 9.
[47] W.M. Shu, E. Wakai, T. Yamanishi, Nucl. Fusion. 47 (2007) 201.
[48] R.A. Causey, T.J. Venhaus, Phys. Scr. T94 (2001) 9.